nature chemistry

ARTICLES

PUBLISHED ONLINE: 14 NOVEMBER 2016 | DOI: 10.1038/NCHEM.2644

Engineering genetic circuit interactions within and between synthetic minimal cells

Katarzyna P. Adamala[1†‡], Daniel A. Martin-Alarcon[2‡], Katriona R. Guthrie-Honea[1] and Edward S. Boyden[1,2,3*]

Genetic circuits and reaction cascades are of great importance for synthetic biology, biochemistry and bioengineering. An open question is how to maximize the modularity of their design to enable the integration of different reaction networks and to optimize their scalability and flexibility. One option is encapsulation within liposomes, which enables chemical reactions to proceed in well-isolated environments. Here we adapt liposome encapsulation to enable the modular, controlled compartmentalization of genetic circuits and cascades. We demonstrate that it is possible to engineer genetic circuit-containing synthetic minimal cells (synells) to contain multiple-part genetic cascades, and that these cascades can be controlled by external signals as well as inter-liposomal communication without crosstalk. We also show that liposomes that contain different cascades can be fused in a controlled way so that the products of incompatible reactions can be brought together. Synells thus enable a more modular creation of synthetic biology cascades, an essential step towards their ultimate programmability.

Chemical systems capable of performing biochemical reactions in the absence of live cells have been used extensively in research and industry to study and model biological processes[1,2], to produce small molecules[3,4], to engineer proteins[5,6], to characterize RNAs[7], as biosensors[8,9] and molecular diagnostic tools[10], and to extend the sensing abilities of natural cells[11]. Organisms from all three domains of life have been used to obtain transcription/translation (TX/TL) extracts for cell-free production of biochemical products from genetic codes[12]. Encapsulating cell-free TX/TL extracts into liposomes creates bioreactors often referred to as synthetic minimal cells (here abbreviated as synells)[13–16]. Although synells have been employed to make functional proteins using encapsulated systems reconstituted from recombinant cell-free translation factors[17–19], as well as cell-free extracts from bacterial[6,20] and eukaryotic cells[21], work on liposomal synells has so far focused on the expression of single genes, with the goal of synthesizing a single-gene product, and within a homogeneous population of liposomes.

Here we confront a key issue in synthetic biology—the modularity of multicomponent genetic circuits and cascades. We show that by encapsulating genetic circuits and cascades within synells (Fig. 1a,b) and orchestrating the synells to either operate in parallel (Fig. 1c), communicate with one another (Fig. 1d) or fuse with one another in a controlled way (Fig. 1e), we can create genetic cascades that take advantage of the modularity enabled by liposomal compartmentalization. Thus, our strategy enables genetic cascades to proceed in well-isolated environments while permitting the desired degree of control and communication. We present design strategies to construct and utilize such synell networks, and thus expand the utility of liposome technology and improve the modularity of synthetic biology. Synell networks may support complex chemical reactions that would benefit from both the high-fidelity isolation of multiple reactions from one another, as well as controlled communication and regulatory signal exchange between those reactions. We show, for example, the controlled fusion of two populations of synells that contain mammalian transcriptional and mammalian translational machinery, which are normally incompatible when combined in the same compartment.

Results

Confinement of genetic circuits in liposomes. Before exploring the control of, and communication with, synells that contain genetic cascades, we first characterized the basic structural and functional properties of individual synells. To characterize the size and functionality of our liposomes, we labelled liposome membranes with red dye (rhodamine functionalized with a lipid tail) and filled the liposomes with cell-free TX/TL extract derived from HeLa cells[22–25], as well as DNA encoding either green fluorescent protein (GFP) or split GFP. Structured illumination microscopy (SIM) images showed that GFP liposomes had a diameter between 100 nm and 1 μm (Fig. 2a), a measurement that we confirmed with dynamic light scattering (DLS, Supplementary Fig. 1). We used flow cytometry to quantify the functional expression of genes by synells; 68.4% of the GFP liposomes expressed fluorescence, along with 61.8% of those that encapsulated split GFP (Fig. 2b–d; Supplementary Fig. 2 shows control flow-cytometry experiments). We characterized the enzymatic activity of several reporters in our liposomes (Supplementary Fig. 3) and used a western blot to provide an additional non-enzymatic characterization of luciferase expression (Supplementary Fig. 4). We compared the performance of mammalian (HeLa) and bacterial (*E. coli*) TX/TL systems in our liposomes, and found the mammalian system to be slower and have a lower protein yield (Supplementary Fig. 5).

Having established that the liposomes were of the proper size and functionality, we next sought to verify that a well-known advantage

[1]Media Lab, Massachusetts Institute of Technology, Cambridge, Massachusetts 02139, USA. [2]Department of Biological Engineering, Massachusetts Institute of Technology, Cambridge, Massachusetts 02139, USA. [3]McGovern Institute for Brain Research, Department of Brain and Cognitive Sciences, Massachusetts Institute of Technology, Cambridge, Massachusetts 02139, USA. †Present address: Department of Genetics, Cell Biology, and Development, University of Minnesota, 5-128 MCB 420 Washington Ave SE, Minneapolis, Minnesota 55455, USA. ‡These authors contributed equally to this work. *e-mail: esb@media.mit.edu

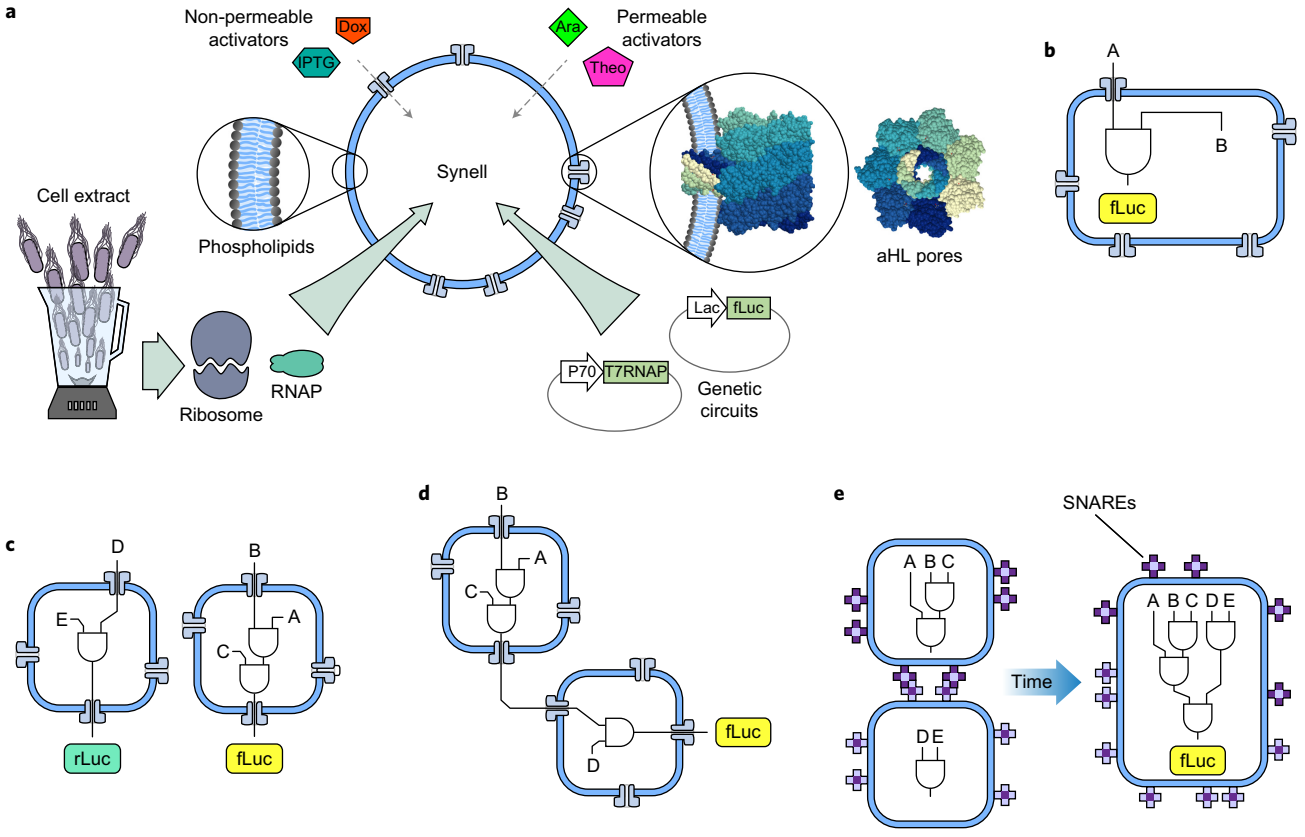

Figure 1 | An overview of genetic circuit interactions within and between synells. a, Synells are semipermeable compartments made from a phospholipid bilayer membrane and various contents. The membrane can display a variety of proteins, including channel-forming proteins such as aHL (grey membrane pores). The phospholipid membranes of synells are permeable to molecules such as theophylline (Theo) and arabinose (Ara), and are permeable to others, such as IPTG and Dox, when aHL channels are present; these molecules can be used to trigger activity within synells. Synells can encapsulate cell lysates with transcriptional and/or translational activity, as well as DNA vectors that encode genes. In this Article, we demonstrate four novel competencies of synells that, together, can be used to create complex, modular genetic circuits. **b**, Synells can contain genetic circuits in which all the components and operations take place within the same liposome. fLuc, firefly luciferase. **c**, Two genetic circuits can work independently in separate liposome populations. rLuc, Renilla luciferase. **d**, Genetic circuits within two different liposome populations can interact. **e**, Genetic circuits can run in parallel in separate compartmentalized reactions; if those reactions are encapsulated by liposomes that carry fusogenic peptides, such as SNAREs, the reaction products can be joined together in a hierarchical fashion. In panels **b**–**e**, the letters A, B, C, D and E represent inputs to genetic circuits (proteins, DNA, small molecules, and so on).

of liposomal compartmentalization—facilitated reaction efficacy caused by molecular confinement (encapsulating reactants within a liposome facilitates their interaction because of the small volume)[26–29]—can help support multicomponent genetic circuits as well as chemical reactions of higher order. We compared cell-free TX/TL reactions that produce firefly luciferase (fLuc) from one, two or three protein components, and tested them in bulk solution versus synells. In this experiment, we used HeLa-cell extract that constitutively expressed the ten–eleven translocation (Tet) protein to mediate small-molecule induction of the transcription of the one, two or three fLuc components, as well as alpha-haemolysin (aHL), which serves as a pore to admit doxycycline (Dox) to trigger Tet function[20,30,31]. The one-component luciferase was simply conventional monolithic fLuc (Fig. 3a); the two-component system (that is, to explore second-order reactions) comprised the two halves of a split fLuc, each attached to a coiled coil and a split intein fragment to bring the halves together and covalently bridge them (Fig. 3b)[32]; and the three-component system involved the halves of split fLuc bearing coiled coils and split inteins, with the coiled coils targeting a third protein, a scaffold (Fig. 3c)[32].

For all three orders of luciferase-producing reactions, the effect of dilution on fLuc expression was weaker for the liposomes than for the bulk solution (Fig. 3d–f; $P < 0.0001$ for the interaction between factors of encapsulation and dilution factor; analysis of variance (ANOVA) with factors of encapsulation and dilution factor; see Supplementary Tables 1–3 for the full statistics and Supplementary Fig. 6 for corresponding experiments under the control of a constitutive P70 promoter). As expected, fLuc expression was proportional to the concentration of Dox added to the external solution, and depended on aHL (Fig. 3g–i show end-point expression after three hours (Supplementary Fig. 7 shows the corresponding expression at a one hour end point, and Supplementary Figs 8–10 for the same reactions in bulk solution)). Liposomes produced lower amounts of fLuc than the same volume of TX/TL extract in bulk solution—probably because of the well-known property of stochastic loading of reagents into liposomes[27,28] ($P < 0.0001$ for the factor of encapsulation in ANOVA with factors of time, encapsulation and order (Supplementary Table 4 gives the full statistics)). For the third-order reaction, we found that liposome encapsulation resulted in an efficacy nearly equal to that of bulk solution (Fig. 3l; $P = 0.1324$ for the factor of encapsulation in ANOVA with factors of time and encapsulation (Supplementary Table 7 gives the full statistics)), whereas for the first-order and second-order reactions the liposomes resulted in lower efficacies (Fig. 3j,k; $P < 0.0001$ for the factor of encapsulation in ANOVAs for both analyses, each with factors of time and encapsulation (Supplementary Tables 5 and 6 give the full statistics)). Thus, molecular confinement in liposomes may help facilitate higher-order reactions that require multiple chemical building blocks to be brought together,

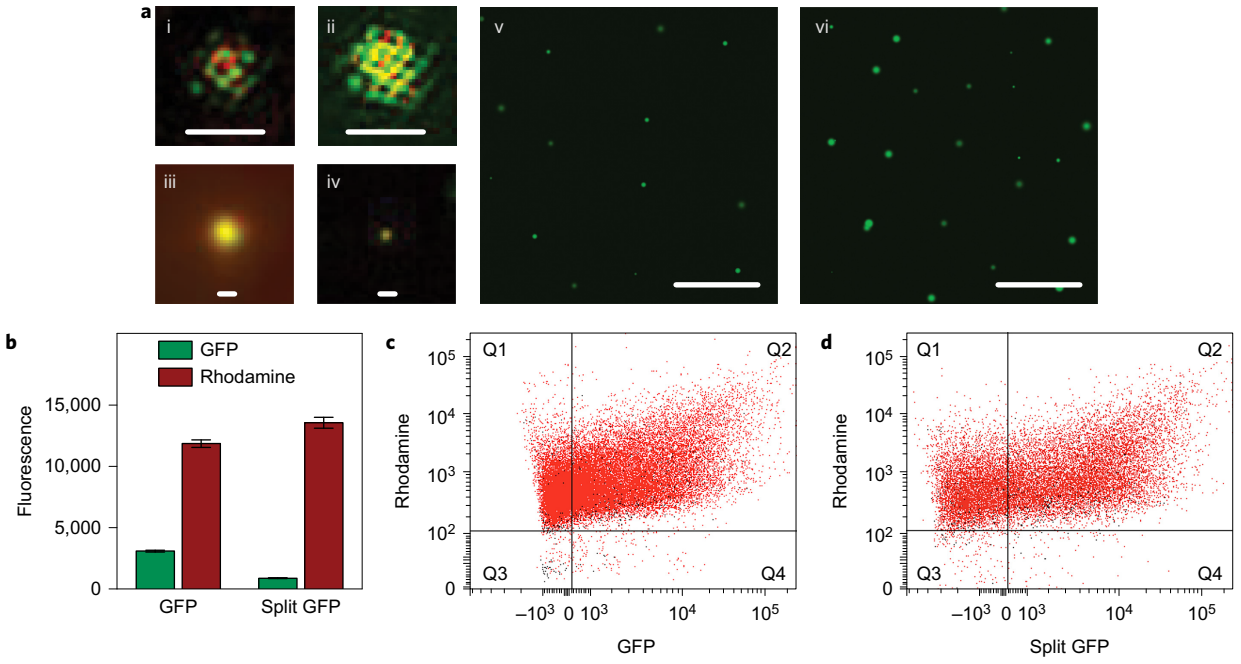

Figure 2 | Molecular confinement of multicomponent genetic cascades. a, Images of liposomes that express GFP. **i–iv**, SIM images of representative liposomes that express GFP and have membranes labelled with rhodamine. Every SIM image (**i–iv**) represents a separate liposome; all the liposomes were imaged on the same day and all the liposomes came from the same sample, prepared 24 h before imaging. All SIM images in this figure are at the same scale. Scale bars, 1 μm (**i** and **ii**) and 200 nm (**iii** and **iv**). **v**,**vi**, Widefield epifluorescent images of liposomes that express GFP. The liposomes for this imaging sample were extruded through a 2 μm filter and dialysed with a 1 μm membrane; **v** shows sample after 6 h incubation and **vi** shows an aliquot of the same sample after 24 h incubation. Scale bars, 10 μm (**v** and **vi**). **b–d**, Fraction of synells that express GFP and split GFP, measured by flow cytometry (Supplementary Fig. 2 shows the control flow-cytometry experiments). **b**, Bulk expression of GFP and fluorescence measured on the sample prior to the flow-cytometry experiments. **c**, Analysis of samples that express GFP; 68.4% of the liposomes produced a measurable green signal. **d**, Analysis of samples that expressed split GFP; 61.8% of the liposomes produced a measurable green signal.

because the restricted movement of reagents increases the probability of the requisite multiway interactions.

Insulation of genetic circuits that operate in parallel liposome populations. As a next step towards engineering sets of liposomes that can communicate with one another, we set out to determine whether liposomes could be used to insulate multiple and potentially incompatible genetic circuits from each other, so that they could operate in the same bulk environment. This insulation would enable modular design; each circuit could be optimized independently and deployed in the same environment as other circuits without interference. These circuits could reuse the same parts (proteins, DNA) for different purposes in different liposomes, and thereby circumvent one limitation of genetic circuits designed for all parts to operate within the same living cell (where one must assume that all the circuit elements might encounter each other and must therefore be inherently orthogonal). Different liposome populations could also contain chemical microenvironments that are not mutually compatible (for example, bacterial and mammalian extracts, or mammalian transcriptional and mammalian translational machinery)—there are numerous examples throughout chemistry of reactions being run under specialized, and thus often isolated, reaction conditions[33].

We first assessed whether multiple liposomal circuits could operate in parallel without crosstalk. To do this, we created populations of liposomes that could respond differently to the same external activator. We built two populations of liposomes carrying mammalian TX/TL extract and the same amount of Dox-inducible luciferase DNA (either Renilla luciferase (rLuc) or fLuc), but varied the amount of aHL DNA to result in high-aHL and low-aHL synell populations (Fig. 4a). High-aHL and low-aHL synells responded to the non-membrane-permeable Dox in the external solution, doing so proportionally to their own aHL concentrations (Fig. 4b). We observed no evidence that Dox acting on one liposome population affected the expression of luciferase in the other population—specifically, there was no significant difference in fLuc expression in high-aHL fLuc liposomes when the rLuc liposomes were high-aHL versus low-aHL, and the same held for the other combinations (Fig. 4b; Sidak's multiple comparisons test after ANOVA with factors of luciferase type and aHL combination (Supplementary Table 8 gives the full statistics, and Supplementary Figs 11 and 12 give the rLuc and fLuc expression data at different aHL plasmid concentrations, for two different time points)). That is, luciferase expression from each liposome population depended only on the amount of aHL DNA present in that population, and not on that of the other population (Fig. 4c–e). This experiment thus not only verifies the independent operation of multiple non-interacting liposomes, but also verifies that multiple liposome populations can be programmed in advance to have varying response levels to a given trigger and, subsequently, in the same internal solution, they can be triggered to function simultaneously.

Communication between genetic circuits that operate in multiple liposome populations. Having established that genetic circuits in separate populations of liposomes could operate independently, we next sought to begin to create controlled communication pathways between populations of synells. In this way we could create a compartmentalized genetic circuit—which, as noted above, may need to be separated from others for reasons of control fidelity, toxicity or reagent tunability—and connect it to other compartmentalized circuits. Although previous work has emphasized the importance of modularity in genetic circuits[34], to

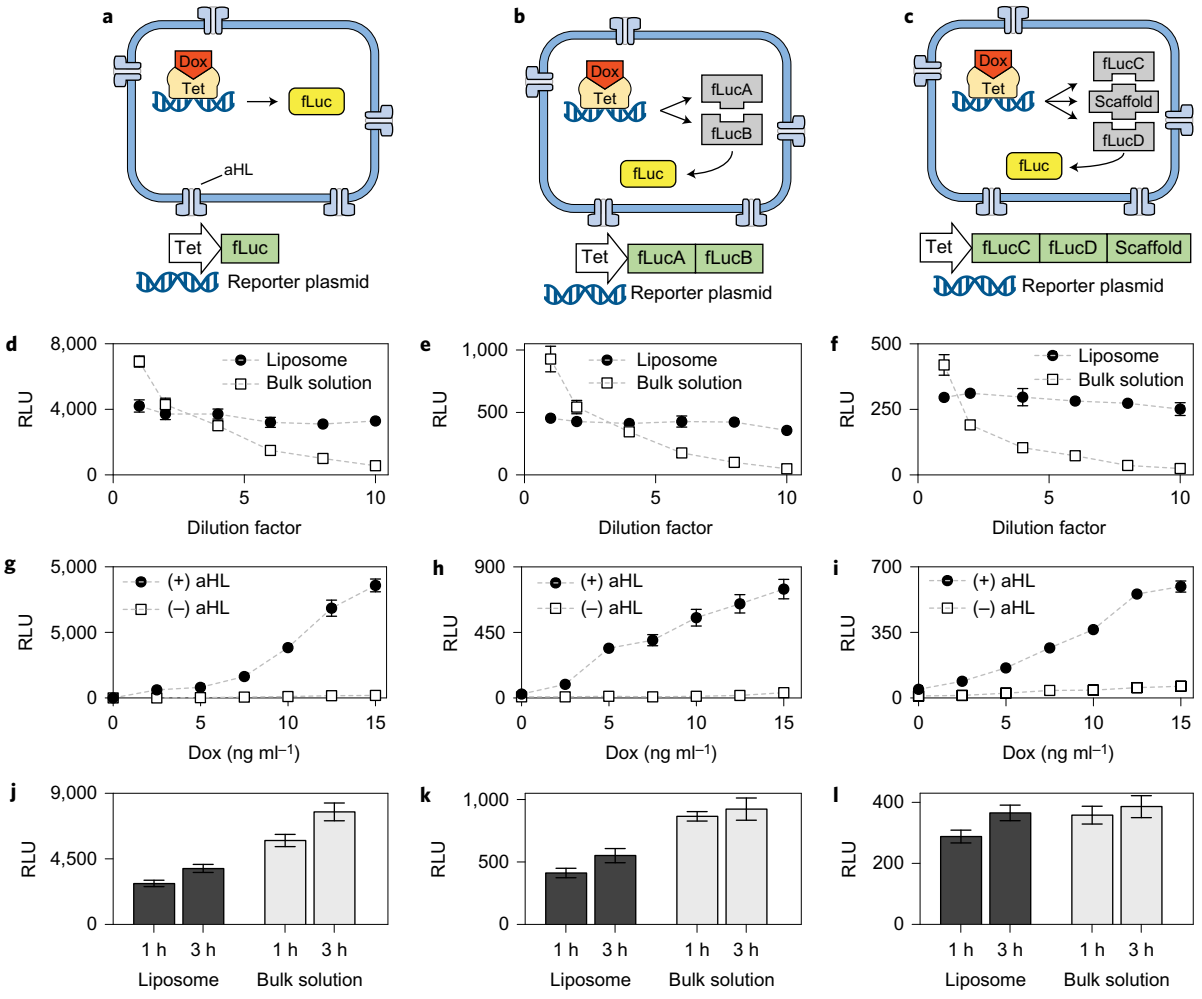

Figure 3 | Comparison of single- and multicomponent genetic circuits. a–c, Genetic cascades that involve one-, two- or three-part luciferase protein assemblies. Expressed under Dox-inducible Tet promoters were whole fLuc (**a**), the two halves (here denoted fLucA and fLucB) of split-fLuc-bearing split inteins and mutually binding coiled coils (**b**) and two halves (here denoted fLucC and fLucD) of split-fLuc-bearing split inteins and coiled coils that bind to a third common template (denoted 'scaffold') (**c**). **d–f**, Effects of dilution on fLuc expression in liposomes versus bulk solution for the fLuc assemblies described in **a–c** (Supplementary Fig. 6 shows the experiments under the control of a constitutive P70 promoter). Dotted lines throughout this figure are visual guides, not fits. **g–i**, End-point expression of luciferase, measured at the 3 h time point, for seven different concentrations of Dox. Supplementary Fig. 7 gives the corresponding 1 h end-point expression data, and Supplementary Figs 8–10 gives these for the same reactions in bulk solution. **j–l**, Comparison of liposomal versus bulk solution expression of luciferase, at two different time points and for 10 ng ml^{-1} of Dox. The two plasmids in **k** and three plasmids in **l** were mixed at equimolar ratios, with the total DNA concentration held constant. Error bars indicate s.e.m., $n = 4$ replicates.

our knowledge nobody has approached the problem by physically separating circuit elements into different liposomes. We built two-component circuits by mixing together two populations of liposomes, a 'sensor' that senses an external small-molecule cue and a 'reporter' that receives a message from the sensor population and produces an output; we could vary the occupancy of each population to achieve a different overall ratio of the two components (Fig. 5a (Supplementary Fig. 13 shows additional characterizations of the membrane-permeable small molecules used throughout Fig. 5a, and Supplementary Tables 9 and 10 give the associated statistics)). Our first version was built with bacterial TX/TL extract (Fig. 5b). The sensor liposomes contained IPTG (isopropyl-β-D-thiogalactoside, a small, non-membrane-permeable activator that induces the *lac* promoter) and the arabinose-inducible gene for aHL (arabinose is membrane permeable, unlike IPTG); these liposomes thus sensed arabinose and released IPTG by expressing aHL channels. We combined these with reporter liposomes that contained constitutively expressed aHL, in which fLuc was under the control of the *lac* promoter—either directly (fLuc under the *lac* promoter) or indirectly (T7RNAP under the *lac* promoter and fLuc under the T7 promoter)—and found that multicomponent compartmentalized genetic circuits thus constructed were able to operate as coherent wholes.

We tested both systems with multiple dilutions of the sensor and reporter liposomes, and found similar dose–response curves from titration of either species of liposome (Fig. 5c,d; bars in these panels represent final time points of six hours; for the complete time series that includes the data in Fig. 5c, see Supplementary Fig. 14; for the end-point expression of the circuit in Fig. 5c without arabinose triggering, see Supplementary Fig. 15; for the complete time series that includes the data in Fig. 5d, see Supplementary Fig. 16; for the end-point expression of the circuit in Fig. 5d without arabinose triggering, see Supplementary Fig. 17). Using this modular architecture, we constructed a genetic circuit that combines both bacterial and mammalian components (Fig. 5e). The sensor liposome in this case responded to theophylline (membrane permeable) to release Dox (non-membrane-permeable). Dox, in turn, activated fLuc expression in the reporter liposomes built with mammalian components. As before, we showed that the multicompartment genetic cascade could function

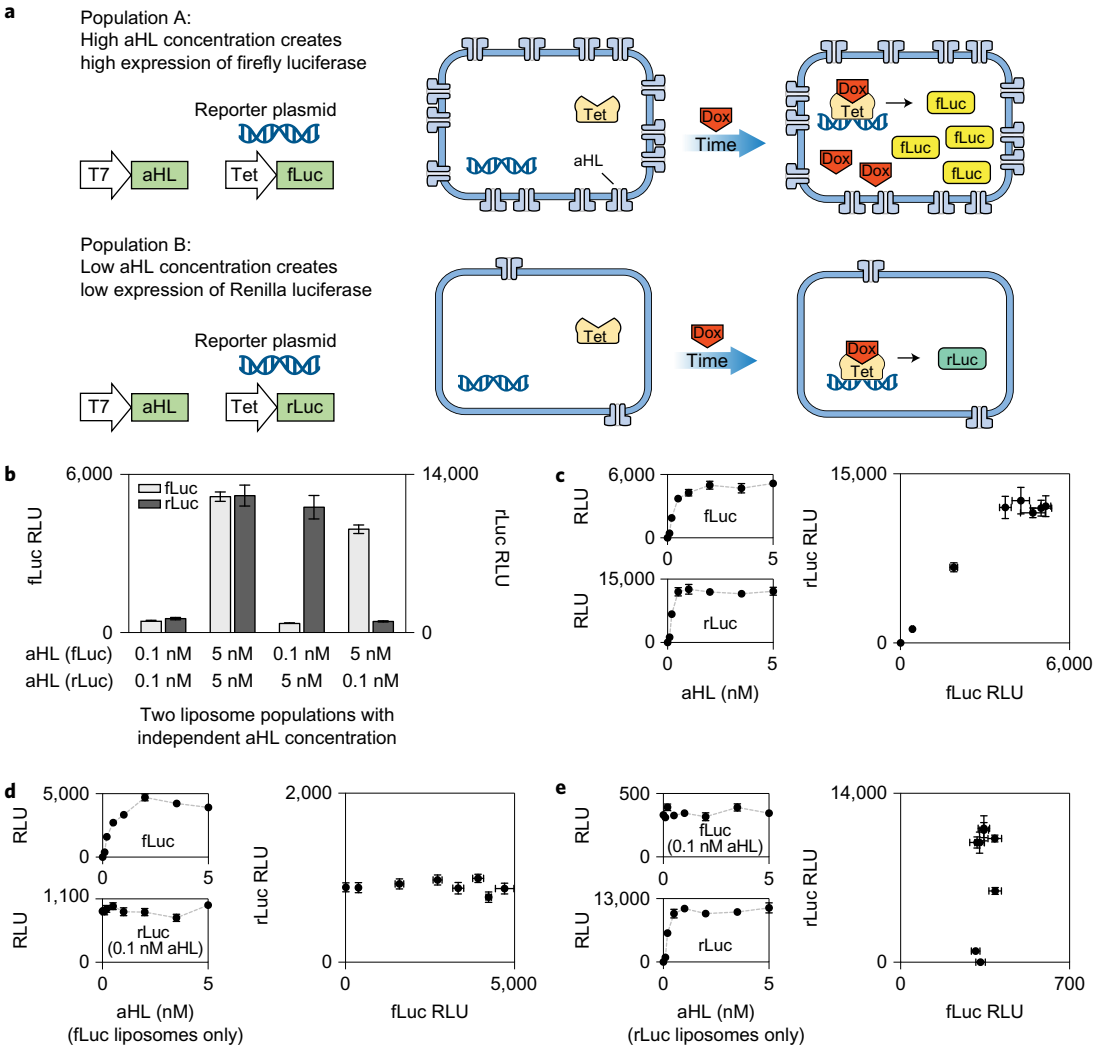

Figure 4 | Insulation of genetic circuits that operate in parallel liposome populations. a, Schematic of liposome populations designed to contain similar genetic components, but to respond differently to the same environmental concentration of the non-membrane-permeable small-molecule activator Dox, by expressing different amounts of the aHL channel protein. These liposomes contain a measured amount of the plasmid for constitutively expressed aHL, and of a plasmid that drives either fLuc or rLuc from the Tet-inducible promoter (the luciferase plasmids were always held at the same concentration). For all the data in this figure, the two populations were incubated together in the solution containing Dox and harvested after 6 h (Supplementary Figs 11 and 12 give the rLuc and fLuc expression as a function of aHL plasmid concentration after 2 and 6 h, respectively). **b**, Each liposome contains either 0.1 or 5 nM of the aHL plasmid. **c**, Luciferase expression in symmetrical populations in which the amount of aHL DNA is the same across the two populations; the amount of fLuc and rLuc expression is shown in the graphs with respect to aHL plasmid concentration and to each other. **d**,**e**, Luciferase expression in asymmetrical populations. **d**, Luciferase expression when Renilla liposomes have a constant aHL plasmid concentration (0.1 nM), but the concentration of that plasmid is varied in the firefly liposomes. The expressions of rLuc and fLuc are shown in the graphs against the plasmid concentration in firefly liposomes and against each other. **e**, Luciferase expression as in **d**, but with constant aHL plasmid concentration in firefly liposomes and variable concentration in Renilla liposomes. Error bars indicate s.e.m., $n = 4$ replicates.

as designed, with similar fLuc expression dose–response curves on titrating either the sensor or reporter liposome concentration (Fig. 5f; bars in this panel represent final time points of six hours; for the complete time series that includes the data in Fig. 5f, see Supplementary Fig. 18; for the end-point expression of the circuit in Fig. 5f without theophylline triggering, see Supplementary Fig. 19). Thus, even multicomponent genetic circuits with different chemical microenvironments (for example, made from bacterial versus mammalian cell extracts) can be assembled into coherent networks that comprise multiple modules.

Fusion of complementary genetic circuits. Finally, having established that it is possible to maintain liposomes in high-integrity states despite being mixed, we sought to engineer synells to fuse so that they could bring together two genetic cascades into the same environment in a programmable fashion. Two precursors might require synthesis in different milieus, but ultimately need to be reacted with one another. One prominent example is that of mammalian transcription and translation. Functionally, mixed mammalian transcription and translation cell-free extracts are not able to result in the transcription of DNA into RNA and then the translation of RNA into protein, perhaps because the microenvironments of the mammalian nucleus and cytoplasm are quite different, which makes their cell-free extracts incompatible (Supplementary Fig. 20). Rather than mixing the two cell-free extracts into a single non-functioning mixture, it might be preferable to use synells to compartmentalize the reactions. Once nuclear-extract synells have completed transcription, it might be desirable to fuse them with cytoplasmic-extract synells for the translation to take place.

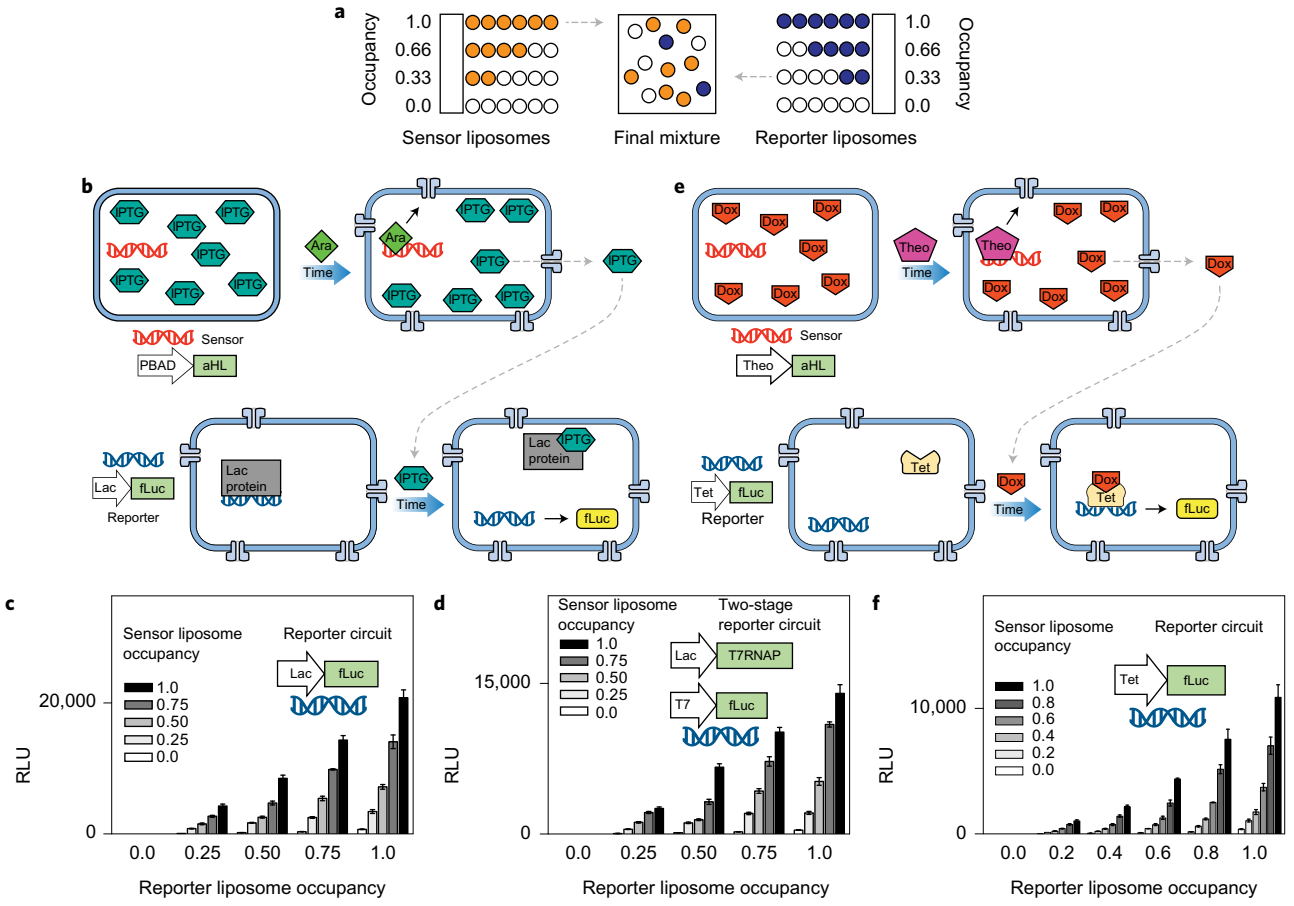

Figure 5 | Communication between genetic circuits that operate in multiple liposome populations. a, Scheme for mixing two populations of liposomes at different ratios of their components while maintaining a constant lipid concentration of 10 mM (the same scheme was used throughout this figure and in Fig. 6). Each population contains the same amount of liposomes, but the liposome occupancy can vary between 0 (all liposomes are empty) and 1 (the maximum fraction of the liposomes contain reagents). **b**–**d**, Externally activated two-part circuits, with bacterial TX/TL. **b**, Scheme of interacting populations, denoted sensor and reporter. Sensor liposomes contain the aHL gene and are filled with IPTG; reporter liposomes contain machinery for fLuc expression. During activation, arabinose (Ara) diffuses through the sensor liposome membrane and induces aHL expression, which releases IPTG, which induces fLuc expression in the reporter. **c**, Expression of fLuc for varying ratios of occupancy (as in **a**) for the sensor and reporter liposomes with the indicated contents. **c** represents the 6 h time point (Supplementary Fig. 14 shows the complete time series and Supplementary Fig. 15 shows this circuit without arabinose). **d**, Expression of fLuc for a circuit in which the reporter liposomes contain DNA for a multicomponent genetic cascade, as indicated. **d** represents the 6 h time point (Supplementary Fig. 16 shows the complete time series and Supplementary Fig. 17 shows this circuit without arabinose). **e**,**f**, Externally activated two-part circuits that contain both bacterial and mammalian TX/TL components. **e**, Sensor vesicles contain the Theo-triggered aHL gene and Dox; reporter liposomes contain constitutively expressed aHL and Tet, and Dox/Tet-driven fLuc. During activation, Theo diffuses through the membrane of the activator liposomes and induces aHL expression, which creates pores that release Dox from the activator. Dox induces fLuc expression in the reporter liposomes. **f**, Expression of fLuc for varying ratios of sensor and reporter liposomes (**f** represents the 6 h time point; Supplementary Fig. 18 gives the complete time series and shows this circuit without Theo). Error bars indicate s.e.m., $n = 4$ replicates.

Thus, we sought to make liposomes capable of controlled fusion (Fig. 6a). Fusing liposomes of opposite charge was previously demonstrated to activate gene expression in liposomes[35]. Our system uses only one kind of membrane composition (POPC (1-palmitoyl-2-oleoyl-*sn*-glycero-3-phosphorylcholine) cholesterol membranes, known to be a good environment for membrane channels such as aHL), so to achieve fusion between liposomes we used SNARE (SNAP receptor (SNAP, soluble *N*-ethylmaleimide-sensitive factor attachment protein))/coiled-coil hybrid proteins (here the hybrid proteins are called SNAREs for short), which can be generated in complementary pairs that are specific in their fusion properties[36,37]. We could thus fuse together complementary circuit elements by encapsulating them in separate populations of SNARE-fusable liposomes. We confirmed that SNAREs mediated liposome fusion through SIM imaging (Fig. 6a) by observing fluorescence resonance energy transfer (FRET) signals from lipid dyes added to the liposome membranes (FRET signals showed that the fusion process takes place within minutes (Supplementary Figs 21 and 22)) and by observing mixing of the liposome content, reported as dequenching of a molecular beacon encapsulated in one population of liposomes by a complementary target encapsulated in the other population (Supplementary Fig. 23). We observed large liposomes and also liposome aggregates (presumably in the process of fusing) of sizes on the order of 5–10 μm, and measured a minimal amount of leakage from the liposomes during the process of fusion (Supplementary Fig. 24).

We tried several combinations of complementary circuit elements: the gene for T7RNAP and a T7-driven fLuc (Fig. 6b); a non-membrane-permeable small-molecule trigger (IPTG) and an IPTG-triggered (*lac*-promoter-driven) fLuc (Fig. 6c); genes for a membrane pore (aHL) and a *lac*-promoter-driven fLuc in an IPTG-containing ambient (Fig. 6d); and two different genes encoding for parts of split luciferase using the same fLucA and fLucB as in Fig. 3b (Fig. 6e). For one final test, liposomes that carried

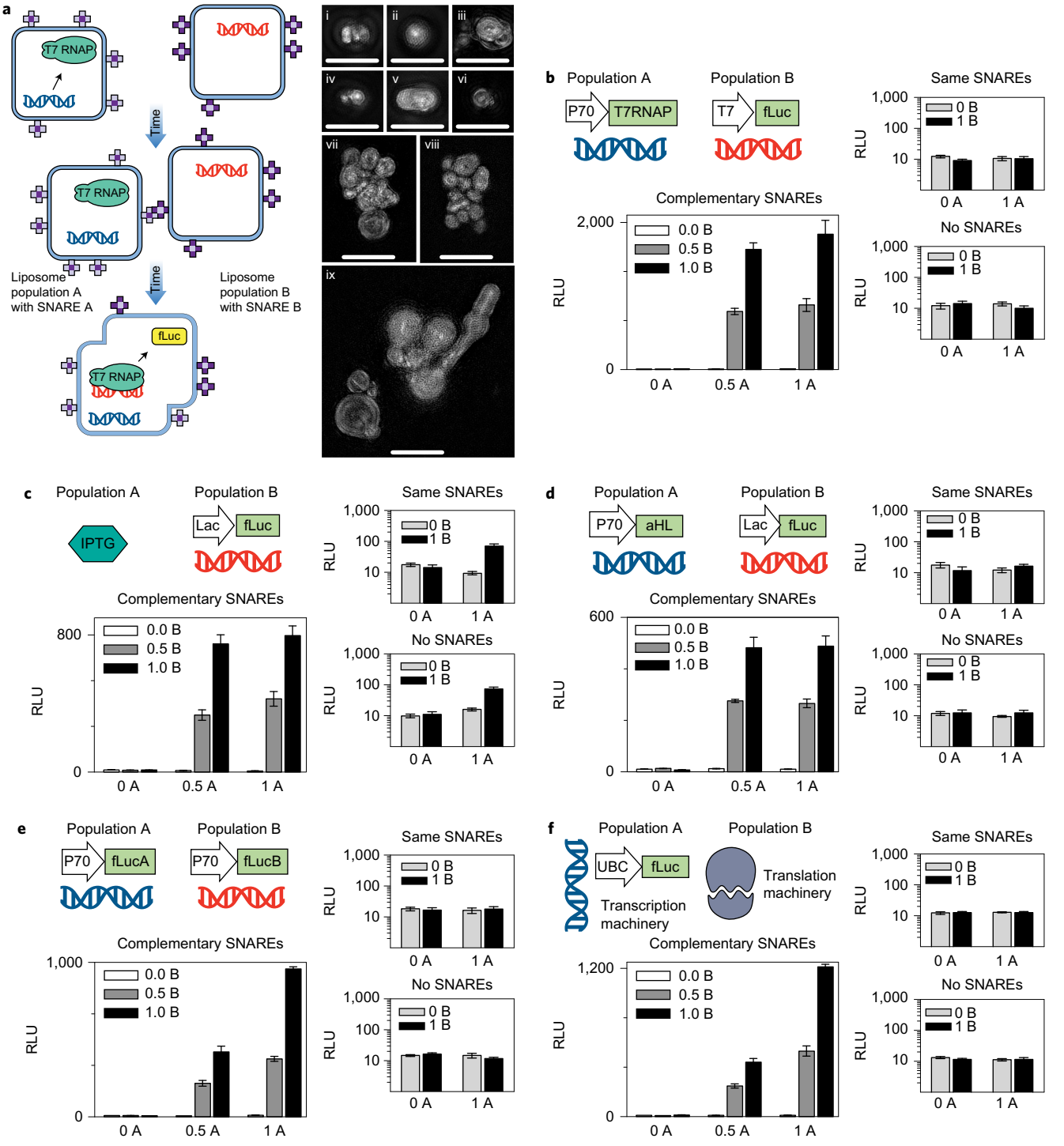

Figure 6 | Fusion of complementary genetic circuits. a, General scheme for SNARE-mediated liposome fusion. We created two populations of liposomes, A and B, decorated with complementary SNARE protein mimics in their outer leaflet. The images to the right, in **i**–**ix**, are maximum-intensity projections of SIM *z*-stacks of liposome membrane labelled with rhodamine, bearing complementary SNARE pairs and fused for 4 h. All the images (**i**–**ix**) represent separate fields of view. Scale bars, 5 μm. All liposomes in this figure, except **f**, contained bacterial TX/TL components. **b**–**f**, Five different types of the liposome fusion concept, exploring several ways to distribute genetic circuits across fusable liposomes, with two different populations of liposomes at three occupancy levels for each case. **b**, Mixing of constitutively expressed T7 RNA polymerase with fLuc under T7 promoter. **c**, Mixing of a non-membrane-permeable small-molecule activator IPTG with its inducible promoter driving fLuc production. **d**, Mixing of a constitutively expressed membrane channel with an inducible promoter driving fLuc production in the background of the small molecule that induces the promoter (IPTG). **e**, Mixing liposomes with genes that encode split protein. **f**, Mixing liposomes that contain a mammalian transcription (HeLa) and translation (HeLa) system, producing fLuc. For all five systems in **b**–**f**, the large graph shows experiments in which the two liposome populations had matching SNAREs, the top small panel is when both liposomes had the same SNARE, and the bottom one when neither population had any SNAREs. In both small graphs of **b**–**f**, the *y* axis is a logarithmic scale to show the near-zero values for non-fusing liposomes. Switching which liposome contained which SNARE had no effect on the results (Supplementary Fig. 25), whereas the absence of SNARE proteins or the presence of identical SNAREs on both populations hindered fusions (small graphs in **b**–**f**). Error bars indicate s.e.m., $n = 4$ replicates.

mammalian nuclear (transcription) extract and the gene for fLuc, incubated for 12 hours, were then mixed with liposomes that contained cytoplasmic (translation) extract, and further incubated for 12 hours (Fig. 6f). We were able to observe the production of fLuc protein, even though a direct combination of transcriptional and translational machinery produced no fLuc above background levels (Supplementary Fig. 20). Throughout all these cases, we observed production of the final output of the genetic cascade only when the two liposome populations were equipped with SNAREs, and only when they were a SNARE cognate pair ($P < 0.0001$ for the factor of SNARE compatibility, ANOVA with factors of mechanism, occupancy and SNARE compatibility (Supplementary Table 11 gives the full statistics; for systems in this figure, switching which liposome contained which SNARE had no effect on the results, as shown in Supplementary Fig. 25)).

Discussion. Liposomes are key in chemistry and chemical biology for compartmentalizing chemical reactions that require different environments or act on different samples. In this work, we show how synells—liposomes containing genes as well as transcriptional and/or translational machinery—enable a great level of modularity for genetic circuit design and execution. We showed that circuits could be designed to run in synell populations in the same container, independent of each other because of the insulation provided by the liposomal membrane. Genetic circuits could also be connected to communicate with one another through small-molecule messengers. This communication was possible even across liposomes that contained incompatible microenvironments, as we showed by constructing the first genetic circuit to contain bacterial and mammalian cell-free extracts and genetic elements. Finally, we explored the use of SNARE mimics to fuse synells together, enabling the direct union of separately synthesized reaction components. Using this strategy, we were able to produce RNA encoding for fLuc in one population of liposomes that contained mammalian transcriptional extract, which on fusion with liposomes that contained mammalian translational extract resulted in protein production—an outcome that does not occur if the gene is simply added to a mixture of the two extracts.

Synells thus enable a new level of modularity for synthetic biology. Modularity is key in engineering, because breaking a complex synthetic biology system into parts that can be independently controlled or regulated, without crosstalk, and that communicate only in well-defined ways, enables each part to be optimized individually while supporting their incorporation into an emergent whole. Our technologies will enable a large number of different synthetic biology problems to be made modular, even those that involve genetic cascades that might interfere with each other (or pose toxicity issues) if they were to all occur in one pot. As our method of compartmentalization is liposomal, there is no need for specialized hardware to mediate the communication and control of multiple interacting reaction systems. Precise temporal control of synell networks could be enhanced even further by using light to trigger optogenetic signalling cascades, which in turn can trigger downstream effects[38,39]. We also show that the molecular confinement of liposomes can facilitate multicomponent protein–protein interactions.

Our synells, in addition to the power they offer to synthetic biology, may also enable the simulation of various complex behaviours that have been proposed as characteristics of early life forms. Controlled communication between cells, the fusion of genetic elements across cells and the assembly of complex genetic cascades towards defined cellular behaviours are all traits that arose in the course of early evolution. Synells have been widely used as models for studying the origin and earliest evolution of life[40–44]. For example, one of us has previously shown that liposomes encapsulating a simple catalyst can be used to model early Darwinian competition mechanisms[41]. Interacting encapsulated genetic circuits will hopefully enable the study of the more-complex characteristics that have been proposed for the last universal common ancestor[45–47], and perhaps help to reveal the dynamic and boundary conditions that underlie the mechanisms of Darwinian evolution[48,49].

Materials

Cloning of expression constructs. The P70 (OR2-OR1-Pr (ref. 50)) and *lac* (Llac-0-1 (ref. 51)) promoter constructs were used in a modified pCI vector (Promega). The original promoter region of the vector was replaced by the appropriate promoter to make our constructs[51]. For bacterial expression, the previously described transcription terminator T500 was added at the end of each ORF (open reading frame). The original untranslated region (UTR) was also removed and replaced with the previously described UTR1 (ref. 50). The mammalian Tet constructs were built into the Tet-On 3G bidirectional vector (Clontech) by cloning the genes into MCS1. The araBAD constructs were built using a PBAD vector[52] (Thermo). We used PBAD–hisB and removed the His-tag and the enterokinase recognition site prior to inserting the genes used in this study.

Flow cytometry with GFP and split GFP. The fluorescence signal from these GFP liposomes was measured after 12 h of incubation for the experiments in Fig. 2b–d. Membranes (red fluorescence) were labelled with Lissamine rhodamine B 1,2-dihexadecanoyl-*sn*-glycero-3-phosphoethanolamine triethylammonium salt (rhodamine DHPE), used at 0.2 molar percentage of the POPC concentration. GFP was expressed from a plasmid with the T7 promoter. The halves of split GFP were fused to complementary coiled coils and expressed from two different plasmids (both with the T7 promoter). For the flow-cytometry analysis, events in two fluorescent channels were analysed: GFP and red fluorescence. Each dataset consists of a minimum of 19,000 events. Figure 2c shows an analysis of liposomes that expressed GFP and Fig. 2d shows an analysis of liposomes that expressed split GFP. The percentage of liposomes that expressed protein was calculated as the percentage of events in the quadrant positive in both the green and red channels (Q2 on both plots). The flow cytometer was not calibrated using size standards, and therefore all the information about the size of the particles in the experiment is approximate. For the detailed size measurements of the liposomes in this work, Supplementary Fig. 1 gives data from the DLS experiments. The flow-cytometry analysis was performed on a FACSCanto II, and the data analysis was performed using a FACSDiva 8.0.

fLuc assays. fLuc activity was assayed using the Steady-Glo Luciferase Assay System (Promega). The protein analysis was performed according to the manufacturer's instructions. The cell lysis protocol was replaced with a modified procedure for lysing liposome-encapsulated expression reactions. The 50 µl liposome reactions were quenched by 10 µl of Quench Mix that contained 0.3% v/v Triton-X100 (to disrupt the vesicles), TURBO DNAse (Thermo; final concentration ~2U per 60 µl; 1 µl used), TURBO DNAse buffer (final concentration ~0.5×, 2.5 µl 10× stock used), RNase Cocktail Enzyme Mix (mixture of RNAse A and RNAse T1, 3 µl per 60 µl reaction (Thermo)). The samples were incubated with the Quench Mix for 15 min at 37 °C. The resulting sample was used directly with the Steady-Glo luciferase assay, according to the manufacturer's instructions.

The result is given in relative light units (RLU) with a 10 s integration time.

Enzyme activity assays. Renilla, NanoLuc luciferase, beta-lactamase, beta-galactosidase and chloramphenicol acetyltransferase activity were assayed using commercially available kits, according to the manufacturer's instructions (Supplementary Information gives the detailed procedures).

***E. coli* cell-free TX/TL extract.** Our *E. coli* cell-free extract was prepared according to the Noireaux Lab protocol, from Rosetta 2 BL21 cells (Novagen)[50,53]. The entire extract preparation was performed in a cold room (4 °C).

HeLa cell-free extract. The HeLa cell-free translation extract was prepared according to a previously published protocol[24]. The entire extract preparation was performed in a cold room (4 °C). For the mammalian *in vitro* transcription, we used the HeLa cell-free nuclear fraction transcription system HeLaScribe (Promega).

SNARE protein mimics. The SNARE protein mimics were chemically synthesized by solid-phase protein synthesis (Genscript). SNARE-A was a fusion of the E3 coiled-coil motif and the transmembrane region of the VAMP2 protein (residues 85–116). SNARE-B was a fusion of the K3 coiled-coil motif with a transmembrane region from the syntaxin-1A protein (residues 258–288), as described before[36]. The SNARE peptide-to-lipid molar ratio used in all the experiments was 1:500.

Liposomes that undergo SNARE-mediated fusion form large aggregates made from multiple starter liposomes[36,37]; this does not affect the results in Fig. 6, but it would probably reduce the molecular confinement effects observed in Fig. 3.

Received 6 December 2015; accepted 12 September 2016; published online 14 November 2016

References

1. Carlson, E. D., Gan, R., Hodgman, C. E. & Jewett, M. C. Cell-free protein synthesis: applications come of age. *Biotechnol. Adv.* **30,** 1185–1194 (2012).
2. Smith, M. T., Wilding, K. M., Hunt, J. M., Bennett, A. M. & Bundy, B. C. The emerging age of cell-free synthetic biology. *FEBS Lett.* **588,** 2755–2761 (2014).
3. Hodgman, C. E. & Jewett, M. C. Cell-free synthetic biology: thinking outside the cell. *Metab. Eng.* **14,** 261–269 (2012).
4. Miller, D. & Gulbis, J. Engineering protocells: prospects for self-assembly and nanoscale production-lines. *Life* **5,** 1019–1053 (2015).
5. Shimizu, Y., Kuruma, Y., Ying, B.-W., Umekage, S. & Ueda, T. Cell-free translation systems for protein engineering. *FEBS J.* **273,** 4133–4140 (2006).
6. Shin, J. & Noireaux, V. An *E. coli* cell-free expression toolbox: application to synthetic gene circuits and artificial cells. *ACS Synth. Biol.* **1,** 29–41 (2012).
7. Takahashi, M. K. *et al.* Rapidly characterizing the fast dynamics of RNA genetic circuitry with cell-free transcription–translation (TX-TL) systems. *ACS Synth. Biol.* **4,** 503–515 (2015).
8. Michener, J. K., Thodey, K., Liang, J. C. & Smolke, C. D. Applications of genetically-encoded biosensors for the construction and control of biosynthetic pathways. *Metab. Eng.* **14,** 212–222 (2012).
9. Vamvakaki, V. & Chaniotakis, N. A. Pesticide detection with a liposome-based nano-biosensor. *Biosens. Bioelectron.* **22,** 2848–2853 (2007).
10. Pardee, K. *et al.* Paper-based synthetic gene networks. *Cell* **159,** 940–954 (2014).
11. Lentini, R. *et al.* Integrating artificial with natural cells to translate chemical messages that direct *E. coli* behaviour. *Nat. Commun.* **5,** 4012 (2014).
12. Zemella, A., Thoring, L., Hoffmeister, C. & Kubick, S. Cell-free protein synthesis: pros and cons of prokaryotic and eukaryotic systems. *Chem. Bio. Chem.* **16,** 2420–31 (2015).
13. Forster, A. C. & Church, G. M. Towards synthesis of a minimal cell. *Mol. Syst. Biol.* **2,** 45 (2006).
14. Brea, R. J., Hardy, M. D. & Devaraj, N. K. Towards self-assembled hybrid artificial cells: novel bottom-up approaches to functional synthetic membranes. *Chem. Pub. Soc. Euro.* **21,** 12564–12570 (2015).
15. Luisi, P. L., Ferri, F. & Stano, P. Approaches to semi-synthetic minimal cells: a review. *Naturwissenschaften* **93,** 1–13 (2006).
16. Stano, P. & Luisi, P. L. Semi-synthetic minimal cells: origin and recent developments. *Curr. Opin. Biotechnol.* **24,** 633–638 (2013).
17. Murtas, G., Kuruma, Y., Bianchini, P., Diaspro, A. & Luisi, P. L. Protein synthesis in liposomes with a minimal set of enzymes. *Biochem. Biophys. Res. Commun.* **363,** 12–17 (2007).
18. Yu, W. *et al.* Synthesis of functional protein in liposome. *J. Biosci. Bioeng.* **92,** 590–593 (2001).
19. Oberholzer, T., Nierhaus, K. H. & Luisi, P. L. Protein expression in liposomes. *Biochem. Biophys. Res. Commun.* **261,** 238–241 (1999).
20. Noireaux, V. & Libchaber, A. A vesicle bioreactor as a step toward an artificial cell assembly. *Proc. Natl Acad. Sci. USA* **101,** 17669–17674 (2004).
21. Stech, M. *et al.* Production of functional antibody fragments in a vesicle-based eukaryotic cell-free translation system. *J. Biotechnol.* **164,** 220–231 (2012).
22. Weber, L. A, Feman, E. R. & Baglioni, C. A cell free system from HeLa cells active in initiation of protein synthesis. *Biochemistry* **14,** 5315–5321 (1975).
23. Wimmer, E. Cell-free, *de novo* synthesis of poliovirus. *Science.* **254,** 1647–1651, (1991).
24. Mikami, S., Masutani, M., Sonenberg, N., Yokoyama, S. & Imataka, H. An efficient mammalian cell-free translation system supplemented with translation factors. *Protein Expr. Purif.* **46,** 348–357 (2006).
25. Mikami, S., Kobayashi, T., Masutani, M., Yokoyama, S. & Imataka, H. A human cell-derived *in vitro* coupled transcription/translation system optimized for production of recombinant proteins. *Protein Expr. Purif.* **62,** 190–198 (2008).
26. Tan, C., Saurabh, S., Bruchez, M. P., Schwartz, R. & Leduc, P. Molecular crowding shapes gene expression in synthetic cellular nanosystems. *Nat. Nanotechnol.* **8,** 602–608 (2013).
27. de Souza, T. P. *et al.* Encapsulation of ferritin, ribosomes, and ribo-peptidic complexes inside liposomes: insights into the origin of metabolism. *Orig. Life Evol. Biosph.* **42,** 421–428 (2012).
28. de Souza, T. P., Fahr, A., Luisi, P. L. & Stano, P. Spontaneous encapsulation and concentration of biological macromolecules in liposomes: an intriguing phenomenon and its relevance in origins of life. *J. Mol. Evol.* **79,** 179–192 (2014).
29. Caschera, F. & Noireaux, V. Integration of biological parts toward the synthesis of a minimal cell. *Curr. Opin. Chem. Biol.* **22,** 85–91 (2014).
30. Stefureac, R., Long, Y. T., Kraatz, H. B., Howard, P. & Lee, J. S. Transport of α-helical peptides through α-hemolysin and aerolysin pores. *Biochemistry* **45,** 9172–9179 (2006).
31. Gouaux, E., Hobaugh, M. & Song, L. α-Hemolysin, γ-hemolysin, and leukocidin from *Staphylococcus aureus*: distant in sequence but similar in structure. *Protein Sci.* **6,** 2631–2635 (1997).
32. Selgrade, D. F., Lohmueller, J. J., Lienert, F. & Silver, P. A. Protein scaffold-activated protein trans-splicing in mammalian cells. **135,** 7713–7719 (2013).
33. Tu, Y. *et al.* Mimicking the cell: bio-inspired functions of supramolecular assemblies. *Chem. Rev.* **116,** 2023–2078 (2016).
34. Del Vecchio, D., Ninfa, A. J. & Sontag, E. D. Modular cell biology: retroactivity and insulation. *Mol. Syst. Biol.* **4,** 161 (2008).
35. Caschera, F. *et al.* Programmed vesicle fusion triggers gene expression. *Langmuir* **27,** 13082–13090 (2011).
36. Meyenberg, K., Lygina, A. S., van den Bogaart, G., Jahn, R. & Diederichsen, U. SNARE derived peptide mimic inducing membrane fusion. *Chem. Commun.* **47,** 9405–9407 (2011).
37. Robson Marsden, H., Korobko, A. V., Zheng, T., Voskuhl, J. & Kros, A. Controlled liposome fusion mediated by SNARE protein mimics. *Biomater. Sci.* **1,** 1046–1054 (2013).
38. Inglés-Prieto, Á. *et al.* Light-assisted small-molecule screening against protein kinases. *Nat. Chem. Biol.* **11,** 952–954 (2015).
39. Boyden, E. S. A history of optogenetics: the development of tools for controlling brain circuits with light. *F1000 Biol. Rep.* **3,** 11 (2011).
40. Hanczyc, M. M., Fujikawa, S. M. & Szostak, J. W. Experimental models of primitive cellular compartments: encapsulation, growth, and division. *Science* **302,** 618–622 (2003).
41. Adamala, K. & Szostak, J. W. Competition between model protocells driven by an encapsulated catalyst. *Nat. Chem.* **5,** 495–501 (2013).
42. Balaram, P. Synthesizing life. *Curr. Sci.* **85,** 1509–1510 (2003).
43. Adamala, K. *et al.* Open questions in origin of life: experimental studies on the origin of nucleic acids and proteins with specific and functional sequences by a chemical synthetic biology approach. *Comput. Struct. Biotechnol. J.* **9,** e201402004 (2014).
44. Ruiz-Mirazo, K., Briones, C. & de la Escosura, A. Prebiotic systems chemistry: new perspectives for the origins of life. *Chem. Rev.* **114,** 285–366 (2014).
45. Glansdorff, N., Xu, Y. & Labedan, B. The last universal common ancestor: emergence, constitution and genetic legacy of an elusive forerunner. *Biol. Direct* **3,** 29 (2008).
46. Woese, C. The universal ancestor. *Proc. Natl Acad. Sci. USA* **95,** 6854–6859 (1998).
47. Theobald, D. L. A formal test of the theory of universal common ancestry. *Nature* **465,** 219–222 (2010).
48. Spencer, A. C., Torre, P. & Mansy, S. S. The encapsulation of cell-free transcription and translation machinery in vesicles for the construction of cellular mimics. *J. Vis. Exp.* **80,** e51304 (2013).
49. Adamala, K., Engelhart, A. E., Kamat, N. P., Jin, L. & Szostak, J. W. Construction of a liposome dialyzer for the preparation of high-value, small-volume liposome formulations. *Nat. Protoc.* **10,** 927–938 (2015).
50. Shin, J. & Noireaux, V. Efficient cell-free expression with the endogenous *E. coli* RNA polymerase and sigma factor 70. *J. Biol. Eng.* **4,** 8 (2010).
51. Lutz, R. & Bujard, H. Independent and tight regulation of transcriptional units in *Escherichia coli* via the LacR/O, the TetR/O and AraC/I1-I2 regulatory elements. *Nucleic Acids Res.* **25,** 1203–1210 (1997).
52. Guzman, L. M., Belin, D., Carson, M. J. & Beckwith, J. Tight regulation, modulation, and high-level expression by vectors containing the arabinose PBAD promoter. *J. Bacteriol.* **177,** 4121–4130 (1995).
53. Sun, Z. Z. *et al.* Protocols for implementing an *Escherichia coli* based TX-TL cell-free expression system for synthetic biology. *J. Vis. Exp.* **79,** e50762 (2013).

Acknowledgements

We thank E. Vasile and F. Chen for help with the SIM microscopy, and G. Paradis and K. Piatkevich for help with the flow-cytometry experiments. We thank N. Kamat and L. Jin for help with troubleshooting the DLS machine. We thank J. Szostak for sharing the liposome encapsulation formula. We thank V. Noireaux, A. Mershin and A. Engelhart for helpful discussions about cell-free TX/TL systems. E.S.B. acknowledges, for funding, the National Institutes of Health (NIH) 1U01MH106011, Jeremy and Joyce Wertheimer, NIH 1RM1HG008525, the Picower Institute Innovation Fund, NIH 1R01MH103910, NIH 1R01NS075421, National Science Foundation CBET 1053233, New York Stem Cell Foundation-Robertson Award and NIH Director's Pioneer Award 1DP1NS087724. D.A.M.-A. acknowledges support from the Janet and Sheldon Razin (1959) Fellowship.

Author contributions

K.P.A. and D.A.M.-A. contributed equally to this work. K.P.A., D.A.M.-A. and K.R.G.-H. performed the experiments. K.P.A., D.A.M.-A. and E.S.B. designed experiments, analysed the data and wrote the manuscript.

Additional information

Supplementary information is available in the online version of the paper. Reprints and permissions information is available online at www.nature.com/reprints. Correspondence and requests for materials should be addressed to E.S.B.

Competing financial interests

K.P.A., D.A.M.-A. and E.S.B. submitted a provisional patent application based on this work.